Conformational Disorder in the Pseudohexagonal Form of Atactic Polyacrylonitrile

Paola Rizzo, Finizia Auriemma,* Gaetano Guerra,† Vittorio Petraccone, and Paolo Corradini

Dipartimento di Chimica, Università di Napoli Federico II, via Mezzocannone, 4, I-80134, Napoli, Italy, and Dipartimento di Chimica, Università di Salerno, I-84081 Baronissi (SA), Italy

Received May 13, 1996; Revised Manuscript Received August 12, 1996[⊗]

ABSTRACT: Accurate wide angle X-ray diffraction measurements for a highly oriented polyacrylonitrile (PAN) fiber suggest the presence, in the pseudohexagonal form of PAN, of sequences with an average periodicity close to 2.4 Å. This is in qualitative agreement with the mean periodicity anticipated by the knowledge of lateral spacing of the pseudohexagonal cell and of the experimental density value. A conformational analysis has allowed location of minimum energy extended conformations for stereoregular and stereoirregular model chains of PAN. The Fourier transforms of these minimum energy extended model chains have been calculated and compared to the experimental X-ray diffraction data. This comparison indicates that the paracrystalline pseudohexagonal phase of PAN is formed by elongated chain stretches, with atactic configuration. The backbone dihedral angles of these atactic stretches in the minimum energy conformation assume values close to 180°, corresponding to r diads, but may present also large deviations from 180°, corresponding to m diads. Where these deviations occur, the length of the projection along the chain axis of the vector connecting the centers of consecutive monomeric units is shorter than 2.5 Å and close to 2.3 Å, giving a mean chain periodicity in a good agreement with the experimental value.

1. Introduction

Several papers have appeared in the literature concerning the packing and the chain conformation in the paracrystalline phase of polyacrylonitrile (PAN).[1−11] It is well-established that PAN, although substantially atactic, with a distribution of triads and pentads following Bernoullian statistics,[12−14] is able to crystallize. Of course, configurationally disordered chains generate highly disordered crystals.

Indeed, the X-ray diffraction patterns of oriented samples of the most common polymorph (pseudohexagonal form) show only two sharp reflections on the equator at $\xi = 0.19$ Å^{-1} and $\xi = 0.33$ Å^{-1} (Miller indices (100) and (110), respectively) indicating a nearly perfect hexagonal arrangement of the chain axes in the *a-b* plane (the distance between the axes of first neighbouring chains being 6.0 Å).[1,3,5,9]

Off the equator, the X-ray diffraction pattern of the polymer presents only diffuse halos:[7,9] (i) two halos centered on the meridian (i.e. at $\xi = 0$) at $\zeta \approx 0.4$ Å^{-1} and 0.8 Å^{-1}, and (ii) a halo centered around $\xi \approx 0.15$ Å^{-1} and $\zeta \approx 0.25$ Å^{-1}.

As far as the mean chain periodicity and conformation of PAN molecules in the pseudohexagonal phase are concerned, some indications come from density data. In fact, the measured densities of conventional PAN samples are in the range 1.17−1.22 g/cm^3.[15,16] It is reported by Lindenmeyer and Hosemann[5] that little variations in density are observed even when crystallization occurs under a variety of conditions. From the knowledge of the lateral packing of the chains (the distance between the axes of first neighboring chains being equal to 6.0 Å, see above) one can calculate that the average distance along the *c* direction per monomeric unit must be 2.31 Å if the density of the crystalline phase is taken equal to 1.22 g/cm^3 and 2.41 Å if the density of the crystalline phase is taken equal to 1.17 g/cm^3. Also, for a mean chain periodicity equal to 2.54 Å (corresponding to a nearly *all-trans* planar chain), a density value equal to 1.11 g/cm^3 would be calculated. These data are in a better agreement, independently of the degree of crystallinity, with periodicity values somewhat smaller than 2.54 Å and close to 2.4 Å. On the other hand, an approximate periodicity along the chain axes of 2.5 Å has been suggested on the basis of the meridional maxima at ζ around 0.4 and 0.8 Å^{-1};[2,3,9] these data were taken as an indication of a nearly zig-zag planar conformation for the chain.

Liu and Ruland,[9] to reconcile the results of the X-ray diffraction studies with the tacticity and density measurements, suggested that, while short isotactic sequences could be accommodated as well in the planar zigzag conformation, long isotactic sequences would reduce the intramolecular energy by kink formation. These kinks would shorten the chains while their *trans* planar portions were kept parallel (but not co-axial) on both sides of the defect. The presence of about 1 kink per 10 monomeric units would increase the density to the experimental value.

In this paper we try to find possible low-energy extended conformations for configurationally disordered model chains of PAN, which could be able to account for the experimental diffraction patterns as well as the experimental density value, without invoking a kink formation.

In particular, in the first section, accurate wide angle X-ray diffraction measurements for a highly oriented PAN fiber are reported. In the second section, a conformational analysis allows location of minimum energy extended conformations for configurationally disordered model chains of PAN: the analysis will be conducted in detail, as an example, on stretches comprising isolated *m* diads or *mm* triads. In the final section, the Fourier transforms of such extended model chains have been calculated and compared to the experimental X-ray diffraction data.

† Università di Salerno.

⊗ Abstract published in *Advance ACS Abstracts,* November 15, 1996.

S0024-9297(96)00699-7 CCC: $12.00

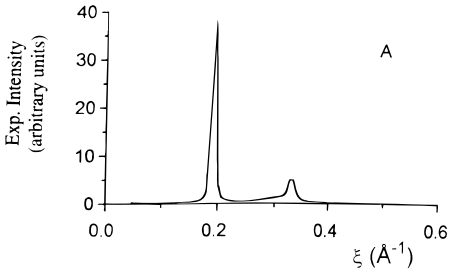

Figure 1. Experimental X-ray diffraction intensity of PAN unannealed fiber, on the equator (along ξ, at $\zeta = 0$).

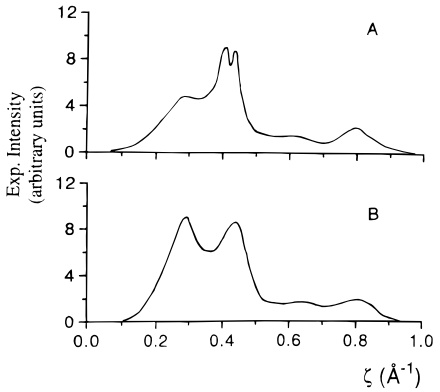

Figure 2. Experimental X-ray diffraction intensity of PAN fiber, on the meridian (along ζ, at $\xi = 0$), when unannealed (A) and annealed (B).

2. Experimental Section

Commercial fibers of PAN, produced by wet spinning from a 14% by weight dimethylacetamide solution and stretching 14 times in a boiling water bath, were supplied by Montefibre of Porto Marghera (Venice, Italy). Analyses were also conducted on this sample after annealing under vacuum at 140 °C for 2 h with free ends. The unannealed and annealed samples correspond to the same (unannealed and annealed) samples as A in ref 17.

Samples suitable for the X-ray diffraction data collections were prepared by filling a Lindemann capillary (diameter of 0.7 mm) with several parallel PAN fibers.

X-ray diffraction spectra were recorded with an automatic diffractometer CAD4 Nonius, always maintaining an equatorial geometry, by using Ni-filtered Cu Kα radiation, in the range $0 < \xi < 0.6$ Å^{-1} with $\Delta\xi = 0.007$ Å^{-1} and in the range $0 < \zeta < 0.9$ Å^{-1} with $\Delta\zeta = 0.002$ Å^{-1}. The diffracted intensities were subtracted for the contribution of the Lindemann capillary; the absorption and polarization corrections were not applied.

Figures 1 and 2 represent the collected intensities along the equator (vs ξ, for $\zeta = 0$) and the meridian (vs ζ, for $\xi = 0$), respectively. Figure 3 shows the X-ray diffraction intensity map $I(\xi,\zeta)$ vs the reciprocal coordinates ξ and ζ. The curves represent the loci points in the reciprocal space ξ,ζ with constant value of the diffraction intensity.

The main features of the patterns of Figures 1−3 are described in the introduction. However, in the patterns of the unannealed sample (Figures 2A and 3) the halo along the meridian at $\zeta \approx 0.4$ Å^{-1} is overlapped by two narrower maxima centered at $\zeta = 0.40$ and 0.43 Å^{-1}. According to Hinrichsen and Orth, the first maximum corresponds to a true meridional reflection with Miller indices (002), and the second one would be the tail of a nearly meridional (202) reflection, both belonging to an orthorhombic form of PAN, which is probably contained in a small amount in our unannealed sample, corresponding to local situations which can be evidenced by electron diffraction.[7,18] As described in ref 17, these two maxima disappear in the annealed PAN samples, and a single broad peak centered at $\zeta = 0.42$ Å^{-1} appears instead (see Figure 2B, redrawn from ref 17). This corresponds to a mean chain periodicity of the chains close to 2.4 Å, in the pseudo-hexagonal phase of PAN. This value of the periodicity accounts for the experimental density value. Furthermore, the presence of a second broad maximum centered around $\zeta = 0.80$ Å^{-1} is apparent, both in part a and b of Figure 2. It is more pronounced for the unannealed PAN sample (Figure 2A), where the (004) reflection of the orthorhombic form[7] also contributes.

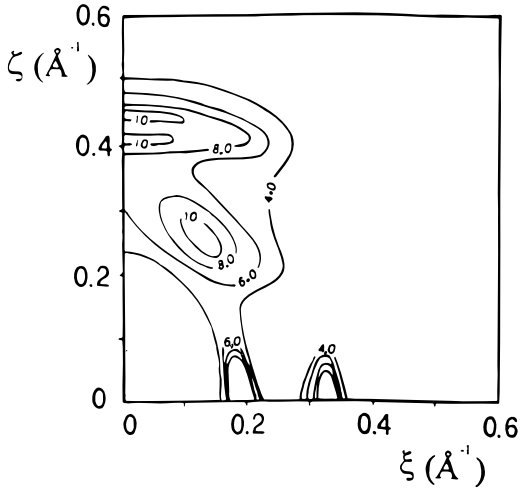

Figure 3. Experimental X-ray diffraction intensity of PAN unannealed sample, vs reciprocal coordinates ξ and ζ. Contour lines with constant $I(\xi,\zeta)$ values are at regular intervals of 2.0.

Table 1. Bond Lengths,[20] Valence Angles, and Bending Constants[21]

bond	d (Å)	angle	τ_o (deg)	$K_{ben} \times 10^2$ (kcal/mol deg^2)
C−C	1.54	C′−C−C′	109.5	3.50
C′−C$_{sp^1}$	1.46	H−C−H	109.5	2.22
C$_{sp^1}$≡N	1.16	H−C−C′	109.5	2.68
C−H	1.09	C−C′−C	109.5	3.50
		C−C′−C$_{sp^1}$	109.5	4.81
		H−C′−C$_{sp^1}$	109.5	2.68
		H−C−C′	109.5	2.68
		C′−C$_{sp^1}$≡N	180	1.52

[a] C and C′ indicate secondary and tertiary carbon sp3 atoms.

3. Conformational Analysis. Methods

The conformational analysis has been performed by keeping, for the sake of simplicity, all the bond distances fixed. The values of bond lengths[20] are listed in Table 1. The hydrogen atoms were explicitly considered. The conformational energy, according to our model, is thus given by the sum of terms:

$$E = \sum E_{ben} + \sum E_{tor} + \sum E_{nb} + \sum E_{el} \qquad (1)$$

where E_{ben} are the energy contributions associated with the deformation of the bond angles τ from the equilibrium value τ_o and are calculated as

$$E_{ben} = \frac{K_{ben}}{2}(\tau - \tau_0)^2 \qquad (2)$$

The values of K_{ben} and τ_o[21] are listed in Table 1.

E_{tor} are the energy contributions associated with torsion angles θ, evaluated according to the method explained in ref 23. With n_X and n_Y being the number of substituents on atoms X and Y for each $X-Y$ bond, the corresponding value of E_{tor} is evaluated as the sum of $n_T = (n_X - 1)(n_Y - 1)$ contributions of the kind

$$\frac{K_{tor}}{2(n_X - 1)(n_Y - 1)}[1 - \cos(n\theta)] \quad (3)$$

with K_{tor} equal to 2.8 kcal/mol and the periodicity n equal to 3.[22]

E_{nb} are the nonbonded energy contributions due to interactions between each couple of atoms separated by more than two bonds, evaluated by terms of the kind

$$E_{nb} = (A/r^{12} - B/r^6) - (A/r_o^{12} - B/r_o^6) \quad (4)$$

where r is the interatomic distance for any couple of nonbonded atoms, A and B are the repulsive and attractive constants, respectively, and r_o is the interatomic distance corresponding to the minimum of E_{nb}. In order to avoid negative contributions, E_{nb} were set equal to 0 for $r \geq r_o$, as explained in ref 23. The values of A and B are those proposed by Sheraga et al. in ref 24 and are listed in Table 2. The C_{sp^1} carbon atom has been treated as C_{sp^2}.

E_{el} are the electrostatic energy contributions, evaluated by terms of the kind

$$E_{el} = q_i\, q_j/(d r_{ij}) \quad (5)$$

with q_i and q_j being the partial charges on atoms i and j, r_{ij} the corresponding distance, and d the dielectric constant. The value of dielectric constant used is 3.5.[25] Partial charges were associated with C_{sp^1} and to N atoms only and placed equal to 0.690 and −0.690 ue, respectively (the dipole moment associated with the C≡N group is 3.9 D[26]).

The analysis of the conformational space is articulated into two steps: (i) calculation of conformational energy maps and geometrical analysis (section 4.1) (contour energy maps were calculated at steps of 10°) and (ii) conformational energy minimizations performed on extended model chains of PAN, selecting the starting conformations from the above maps (section 4.2).

The energy minimization procedure of section 4.2 has been carried out on extended models of stereoregular chains (isotactic and syndiotactic) as well as stereoirregular chains (consisting of *rrrmrr* or *rrmmrr* eptads, as an example). In the energy minimizations, all valence and dihedral angles were considered variable with the exception of the C−C′≡N valence angle, which was rigidly kept constant at a value of 180°.

In order to avoid that the selected extended conformations collapse to coiled chains during the minimization procedure, the following constraint was introduced. The mean periodicity of the chains is kept larger than a minimum value arbitrarily fixed equal to 2.2 Å by adding a fictious energy contribution to eq 1. The last value was set equal to zero, when the end to end distance of the eptamer was higher than 7 × 2.2 Å, and was calculated according to the equation of a parabola ($y = kx^2$), when the end to end distance was lower than 7 × 2.2 Å. The spring constant k was set arbitrarily equal to 100 kcal/(Å^2 mol), x being the absolute value of the displacement of the end to end distance from the minimum value.

In order to be sure that the final conformation obtained through the minimization is a true minimum, at least three independent minimizations were carried out, starting from different conformations placed inside the same minimum of the conformational energy map.

Table 2. Attractive and Repulsive Terms and Sum of the Van der Waals Radii for all the Considered Couples of Nonbonded Atoms (from ref 24)

atoms	A (kcal Å^{12}/mol)	B (kcal Å^6/mol)	r_0 (Å)
C−C	2.86×10^5	3.71×10^2	3.4
C−H	3.81×10^4	1.28×10^2	2.9
C−C1	2.84×10^5	5.29×10^2	3.2
C−N	2.16×10^5	3.66×10^2	3.25
H−H	4.47×10^3	4.68×10	2.4
H−C1	3.64×10^5	1.89×10^2	2.7
H−N	2.70×10^4	1.25×10^2	2.75
C1−N	2.09×10^5	5.20×10^2	3.05
C1−C1	2.80×10^5	7.67×10^2	3.0
N−N	1.61×10^5	3.63×10^2	3.1

Scheme 1. Model Chains Used in the Calculations: (A) Isotactic, (B) Syndiotactic, (C) *rrrmrr* Eptad, and (D) *rrmmrr* Eptad[a]

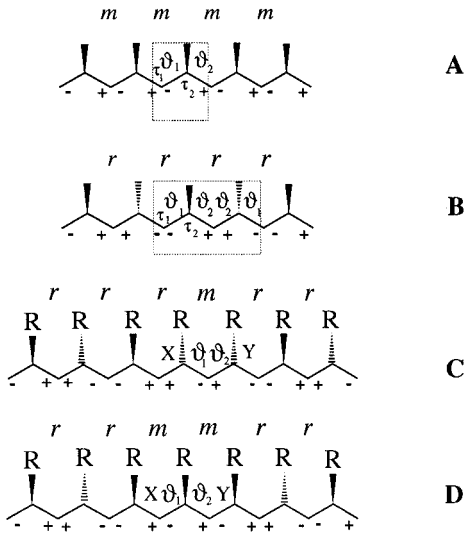

[a] The configurations of the bonds of the backbone and the dihedral angles which have been varied in our calculations are indicated. τ_1 and τ_2 indicate the backbone bond angles.

4. Conformational Analysis. Results

The aim of this section is to analyze the energetical feasibility of extended chains of atactic PAN, suitable for the packing in the crystalline pseudohexagonal form.

In particular, the present analysis mainly concerns stereoirregular model chains consisting of *rrrmrr* and *rrmmrr* eptads (parts C and D of Scheme 1, respectively). For comparison, calculations are reported also for isotactic (Scheme 1A) and syndiotactic (Scheme 1B) model chains.

Following IUPAC rules,[27] conformations referring to torsion angles of the main chain atoms are described as *gauche* (G) or *anticlinal* (A) for torsion angles within ±30° of, respectively, ±60° and ±120°. The symbols G^+ and G^- (or A^+, A^-) refer to torsion angles of similar type but opposite sign.[28] Moreover, we use the symbols T, T^+, and T^- to describe the nearly *trans* conformations with torsion angles within ±10° of, respectively, 180°, 160°, and −160°.

For our purposes, it is useful to distinguish from a configurational viewpoint as (+) or (−) the bonds of the chain which are adjacent to the carbon atoms constituting the stereoisomeric centers.[28] We recall that, in vinyl polymers, the (+) bonds tend to assume G^+ or T conformations whereas (−) bonds tend to assume G^- or T conformations.[28]

Starred A, G, or T symbols indicate that, for the considered minimum energy conformation, the sign of the value of the dihedral angle is opposite with respect

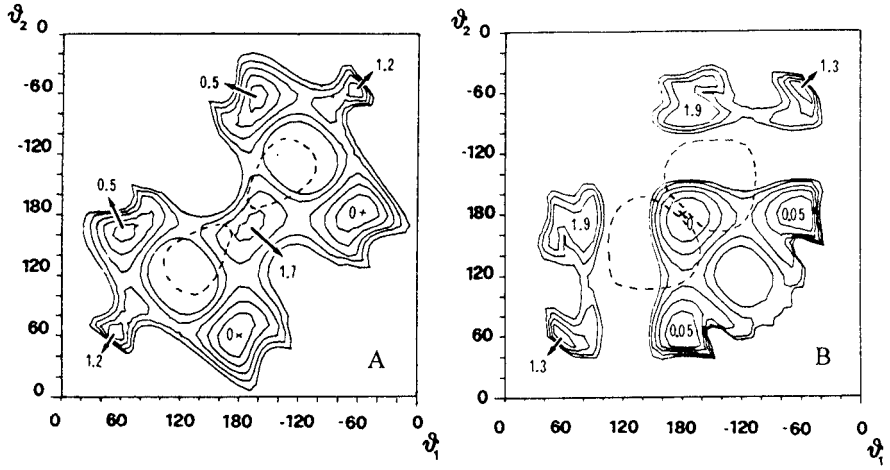

Figure 4. Conformational energy maps for the stereoregular PAN as a function of θ_1 and θ_2, of the (A) isotactic model chain (Scheme 1A) and (B) syndiotactic model chain (Scheme 1B). The curves are reported at intervals of 2 kcal/mol of monomeric units with respect to the absolute minimum; the values of the energies corresponding to the minima are indicated. The dashed curve corresponds to the loci points θ_1 and θ_2, for which the unit height is equal to 2.4 Å (A) and 4.8 Å (B).

Table 3. Results of the Conformational Energy Minimization Procedure for the Syndiotactic and Isotactic Model Chains

symbol[a]	ΔE^b (kcal/mol)	dihedral angles (deg)	h^c Å
	Syndiotactic Model Chain		
|TT|TT|	0	177, 177, −177, −177	2.54
	Isotactic Model Chain		
|TT|TT|	3.0	180, 180, 180, 180	2.54
$\|T^+T^{+*}\|T^{-*}T^-\|$	2.8	157, 161, −161, −166	2.54

[a] Starting conformation for the minimization procedure. [b] Minimized conformational energy per monomeric unit. [c] The unit height of the chain.

to the configurational sign of the corresponding bond. For instance, the symbol G^{-*} indicates a dihedral angle close to −60°, for a (+) bond.

4.1. Conformational Energy Maps and Geometrical Analysis. For the isotactic and syndiotactic model chains of PAN, only regular conformations have been taken in consideration, starting from the classical sequences of dihedral angles ...$|\theta_1\theta_2|\theta_1\theta_2|$... and ...$|\theta_1\theta_1|\theta_2\theta_2|\theta_1\theta_1|\theta_2\theta_2|$..., respectively, where the vertical bars limit the dihedral angles defined between a couple of consecutive tertiary carbon atoms (i.e. inside a diad).

Parts A and B of Figure 4 represent the energy contour maps $E(\theta_1,\theta_2)$, vs θ_1 and θ_2, minimizing the energy with respect to the valence angles τ_1 and τ_2 (defined in the parts A and B of Scheme 1 and initially placed equal to 113° and 111°, respectively). The energies are relative to one mole of monomeric units. The dashed curves superimposing the continuos curves in parts A and B of Figure 4 are the loci points θ_1 and θ_2, whereby the unit height h is equal to 2.4 or 4.8 Å, respectively.

In agreement with previous energy analyses,[10,11,26] extended conformations of isotactic model chains of PAN do not correspond to conformational energy minima. In particular, extended conformations close to the *trans*-planar one present conformational energies at least 3 kcal/mol higher than the absolute minimum (corresponding to TG sequences). On the contrary, for syndiotactic model chains of PAN, the *trans*-planar conformation corresponds to the absolute minimum (see Table 3).

We have also calculated the conformational energy map of isotactic PAN by assuming sequences of dihedral angles ...$|\theta_1\theta_1|\theta_2\theta_2|$.... Conformations with ...$|\theta_1\theta_1|\theta_2\theta_2|$... = ...$|T^+T^{+*}|T^{-*}T^-|$... are enclosed inside a contour energy level 2.8 kcal over the absolute minimum (see Table 3), in agreement with the calculations of Hobson and Windle in refs 10 and 11 (Hobson and Windle[10,11] describe the resulting chains as "emulating the shape and the axial repeat of an equivalent (planar zigzag) syndiotactic molecule").

For the considered stereoirregular model chains consisting of *rrrmrr* and *rrmmrr* sequences, the dihedral angles which are varied for the construction of the energy maps are located around the *m* diads, as shown in the Scheme 1C,D. The sequence of these dihedral angles can be indicated as $X|\theta_1\theta_2|Y$ and as $|X\theta_1|\theta_2Y|$ for the models of parts C and D of Scheme 1, respectively.

In particular, conformational maps vs θ_1 and θ_2, for various values of the dihedral angles X and Y, by keeping all the remaining dihedral angles in the *trans* state and maintaining fixed all the valence angles, have been calculated. The values of X and Y have been fixed equal to 60°, 120°, 150°, 180°, −150°, −120°, and −60°. The zero of the energy in all the maps corresponds to the absolute minimum for the same chain obtained by minimizing the conformational energy also with respect to all the dihedral and valence angles.

Analogous geometrical maps $\Omega(\theta_1,\theta_2)$ have been also constructed, where Ω is defined as the angle between the vector passing through the third and the first atoms and the vector passing through the third-last and the last atoms of the chain backbone. Extended chains correspond to $\Omega = 180°$.

On the basis of these energy and geometrical maps, extended conformations, suitable as starting points of the energy minimization procedures of the next section, have been selected. In particular, for all the constructed maps, possible conformations with $\Omega > 155°$ and $E <$ 10 kcal/mol have been located.

For the case of *rrrmrr* stretches (Scheme 1C), one of the $E(\theta_1,\theta_2)$ maps is shown, as an example, in the Figure 5 for the sequence $T|\theta_1\theta_2|T$. The dashed line in fig 5 represents the loci points θ_1,θ_2 with $\Omega = 155°$ and includes extended conformations having $\Omega > 155°$. The stars indicate some of the extended conformations selected as starting points for the minimization procedures.

The lower energy extended conformations for the case of an *rrrmrr* sequence, localized with the above proce-

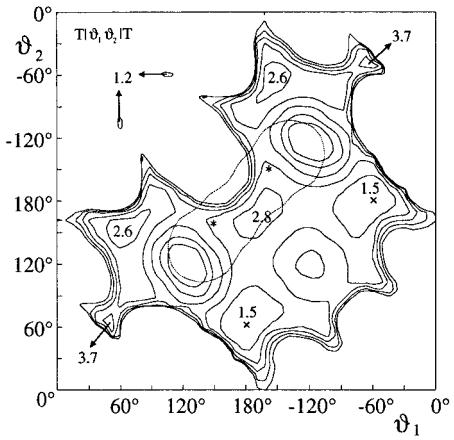

Figure 5. Conformational energy map for the stereoirregular PAN chain, for the *rrrmrr* eptad (Scheme 1C) as a function of θ_1 and θ_2, for $X = Y = 180°$. The curves are reported at intervals of 2 kcal/mol of monomeric units with respect to the absolute minimum; the values of the energies corresponding to the minima are indicated. The dashed curve corresponds to the loci points θ_1 and θ_2, for which the angle Ω (between the axes of the terminal *trans*-planar portions of the chains) is equal to 155° and includes conformations having $155° \leq |\Omega| \leq 180°$.

Table 4. Results of the Conformational Energy Minimization Procedure for a *rrrmrr* Eptad

	...*rrrmrr*...	ΔE^a (kcal/mol)	$X-\theta_1-\theta_2-Y$ (deg)	h^b (Å)
A	T|T$^-$T|T	1.7	177, −169, 172, −179	2.50
B	T$^+$|G$^+$*T|T	1.7	153, 73, 173, −172	2.35
C	T$^+$|G$^+$*T|T$^-$	3.0	152, 72, 176, −154	2.39

[a] Minimized conformational energy per mole of eptamer, over the absolute unconstrained minimum. [b] The average periodicity of the chain having 7 mu.

dure using maps analogous to those of Figure 5, are listed in column 1 of Table 4.

Analogously, for the case of *rrmmrr* stretches (Scheme 1D), four representative conformational maps are shown, as an example, in the Figure 6A−D. As in Figure 5, the dashed lines are the loci points θ_1,θ_2 with $\Omega = 155°$ and the stars indicate some of the extended conformations selected as starting points for the minimization.

The lower energy extended conformations for the case of an *rrmmrr* sequence localized with the above procedure using maps analogous to those of Figure 6, are listed in column 1 of Table 5.

4.2 Conformational Energy Minimizations. In this section the results of the energy minimizations, assuming as starting points the sequences of conformations shown in the Tables 4 and 5, are presented.

For the isotactic and syndiotactic models, the results of the conformational energy minimization procedure (conformational energy per monomeric unit, dihedral angles, and the periodicity *h* along the chain axis) are reported in Table 3. Of course, unlike the case of the syndiotactic configuration, for which the extended chain corresponds to the absolute minimum of the conformational energy, for the completely isotactic configuration the nearly *trans*-planar conformation implies an energy cost of about 3 kcal/mol above the absolute minimum per mol of monomeric unit, for both the *trans*-planar chain with $\theta_1 = \theta_2 = 180°$ and the Hobson-like chain[10,11] with ...$|\theta_1\theta_1|\theta_2\theta_2|$... = ...|T$^+T^+$*|T$^-$*T$^-$|....

The results of the energy minimization procedures for the model chains with stereoirregularities are reported in Tables 4 and 5. In particular, we report for each conformation, the calculated conformational energies, the corresponding values of the dihedral angles X, θ_1, θ_2, and Y, and the mean length of the projection of the monomeric unit along the chain axis, h, after the minimization.

For the case of a *rrrmrr* configurational sequence (Table 4), the minimization procedure leads to energetically feasible straight chains with small lateral encumbrance for the nearly *trans*-planar conformation (T|TT|T) (Figure 7A). Conformations comprising dihedral angles in a *gauche* state, also at a low cost of conformational energy, may be considered as locally straight with a waviness that we consider as probably digestible in the lattice, as shown in Figure 7A−C.

This analysis, hence, indicates that isolated *m* diads are easily accommodated in crystalline regions: the nearly *trans* conformers do not shorten the mean chain periodicity too much from 2.54 Å, whereas conformers including a G* have a shorter mean chain periodicity, close to 2.4 Å.

For the case of a *rrmmrr* eptad (Table 5), the minimization procedure leads to energetically feasible straight chains with small lateral encumbrance for several local conformations (conformational energy lower than 2−5 kcal/mol). A side view of chain stretching belonging to these seven minimum energy extended conformations are shown in Figure 8A−G.

This analysis, hence, suggests that isolated *mm* triads are easily accommodated in crystalline regions including nearly *trans*-planar chain of PAN. In this case, several sequences of dihedral angles, around the *m* diads, which are energetically feasible, shorten somewhat the mean periodicity of a syndiotactic chain (the corresponding value of *h* in Table 5 are, in fact, in the range 2.4−2.3 Å).

It is worth noting that portions of chains of PAN modeled according to the sequence of dihedral angles listed in Tables 4 and 5 corresponding to *rrrmrr* or *rrmmrr* eptads can be variously combined along the same chain through joints in a nearly *trans* state and still maintain a nearly extended chain at a low cost of free energy.

The presence of a G* rotates the mean plane of the backbone chain of nearly 120°, with the result that the CN side groups project perpendicularly to the chain axis along directions placed at 120° each other. The conformers of Tables 4 and 5 represent only partial solutions to the problem of modeling extended chain conformations of atactic PAN. It is also worth noting that isotactic chains in a regular conformation $(|T^+T^-|G^-*T^-|)_n$ or $(|T^-T^+|G^+*T^+|)_n$ correspond to highly extended chains in a local minimum of the conformational energy, as it has been proposed for the case of isotactic polystyrene.[29]

5. Fourier Transform. Method

Fourier transform calculations are performed on configurationally ordered and disordered chain models, in different conformations.

The Fourier transform of isolated chains can be advantageously compared to the diffracted intensity far from the equator, when there is a low degree of rotational (around the chain axis) and translational (along the chain axis) order between adjacent parallel chains. Near the equator the comparison is, instead, less significant, since also interferences between adjacent chains should be accounted for.

The X-ray diffraction intensity by fibers is conveniently calculated as a function of the reciprocal space

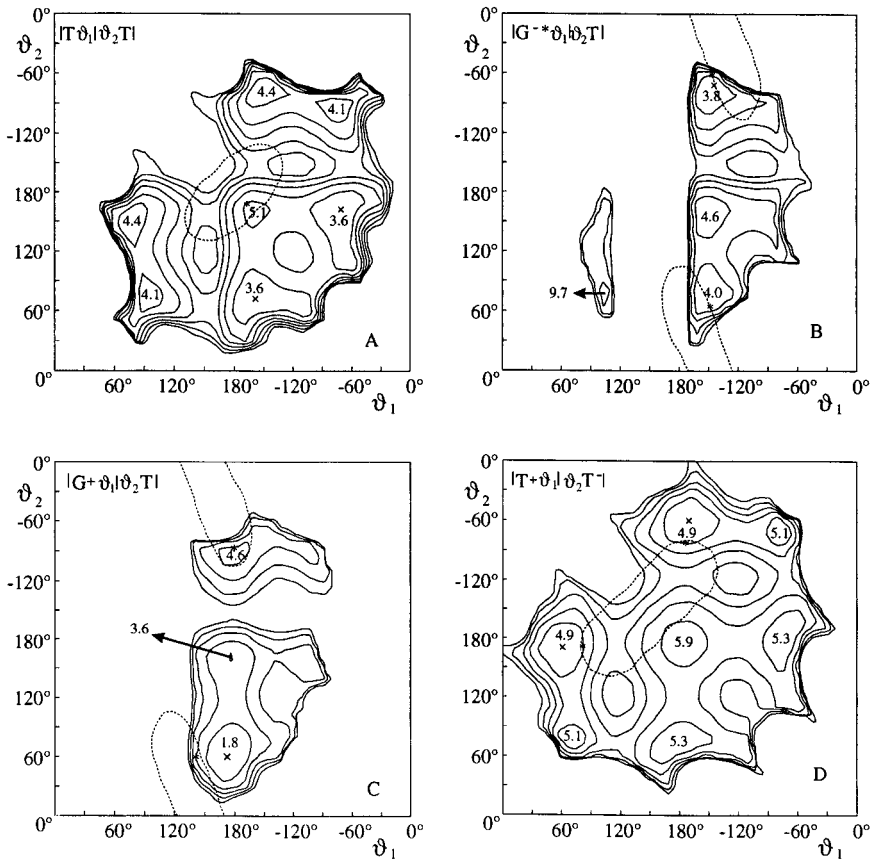

Figure 6. Conformational energy maps for the stereoirregular PAN chain, for the *rrmmrr* eptad (Scheme 1D) as a function of θ_1 and θ_2, for (A) X = T and Y = T, (B) X = G$^-$* and Y = T, (C) X = G$^+$ and Y = T, and (D) X = T$^+$ and Y = T$^-$. The curves are reported at intervals of 2 kcal/mol of monomeric units with respect to the uncostrained absolute minimum; the values of the energies corresponding to the minima are indicated. The dashed curves correspond to the loci points θ_1 and θ_2, for which Ω = 155°, and includes conformations having 155° ≤ |Ω| ≤ 180°.

coordinates ξ, ϕ, and ζ as:

$$I(\xi,\phi,\zeta) = F(\xi,\phi,\zeta)\, F^*(\xi,\phi,\zeta) \qquad (6)$$

where $F(\xi,\phi,\zeta)$ is the structure factor and the * denotes the complex conjugate. For the calculation of the diffraction intensity by an isolated chain cylindrically averaged over the reciprocal coordinate ϕ, we have followed the treatment reported by Tadokoro in ref 30 for the calculation of the molecular structure factor of nonhelical molecules. This treatment leads to the formula for the calculation of the X-ray diffraction intensity, I_c (uncorrected for the polarization and the absorption):

$$I_c(\xi,\zeta) = \sum_{a=1}^{N}\sum_{b=1}^{N} f_a\, f_b J_0(2\pi\xi r_{ab}) \exp -[2\pi i\zeta(z_a - z_b)] \exp(-2\pi^2\zeta^2 u_\zeta^2 |z_a - z_b|/\Delta) \qquad (7)$$

with f_a and f_b being the atomic scattering factors of the ath and bth atoms, N the total number of carbon atoms in the chain, $J_0(2\pi\xi r_{ab})$ the 0th order Bessel function, r_{ab} the distance in the $x-y$ plane between the ath and bth atoms, and z_a and z_b the z coordinates of those couple of atoms. The factor u_ζ^2 in the exponential term represents the mean square displacement of the coordinate z of the atoms, whereas Δ is a parameter having the dimension of a distance, scaling u_ζ^2. The factor $\exp(-2\pi^2\zeta^2 v_\zeta^2|z_a - z_b|/\Delta)$ reduces the interference between each couple of atoms; this reduction increases with an increase of the distance along z of each couple of atoms, hence corresponding to a paracrystalline disorder. For the derivation of this last term, see ref 31.

Table 5. Results of the Conformational Energy Minimization Procedure for a *rrmmrr* Eptad

	...*rrmmr*...	ΔE^a (kcal/mol)	$X-\theta_1-\theta_2-Y$ (deg)	h^b (Å)
A	TT$^-$|T$^+$T	3.6	177, −170, 167, 180	2.49
B	G$^-$*A$^-$|G$^-$*T	2.2	−60, −142, −70, −178	2.37
C	G$^+$T|G$^-$*T	3.2	62, −178, −87, 179	2.39
D	G$^+$T$^+$*|G$^+$T	2.6	57, 150, 61, 180	2.35
E	T$^+$G$^+$*|TT$^-$	5.0	154, 82, 173, −152	2.43
F	T$^+$G$^+$*|T$^+$T	3.3	156, 60, 153, −174	2.37
G	T$^+$T$^-$|G$^-$*T	2.7	165, −159, −71, −174	2.36

[a] Minimized conformational energy per mole of eptamer, over the absolute unconstrained minimum. [b] The average periodicity of the chain having 7 mu.

The reported Fourier transform calculations refer to models including 10 monomeric units. In order to avoid the presence of the subsidiary maxima flanking the main diffraction peaks along the calculated meridional profile due to the finite length of the considered chains, at least for $\zeta \geq 0.20$ Å^{-1}, the interference of only the atoms of the central monomeric unit in the decamer with all the remaining atoms was considered (i.e. in eq 7 one of the summation ranges only over the labels of the atoms belonging to a central monomeric unit) and the value of u_ζ^2/Δ was fixed equal to 0.05 Å. The last setting also produces a broadening of the meridional maxima; the broadening increases with an increase of the ζ value in better semiquantitative agreement with the experimental pattern. For the sake of simplicity,

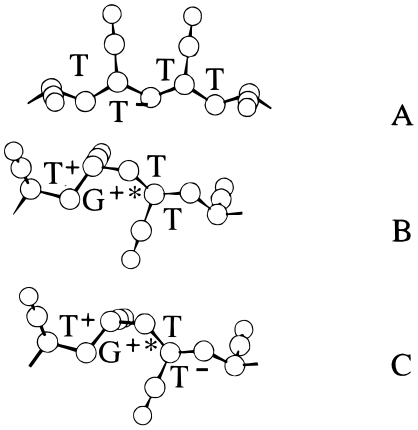

Figure 7. Side views of the chain stretches, with an isolated *m* diad between *r* diads in the minimum energy conformations: (A) T|T⁻T|T, (B) T⁺|G⁺*T|T, and (C) T⁺|G⁺*T|T⁻(see Table 4).

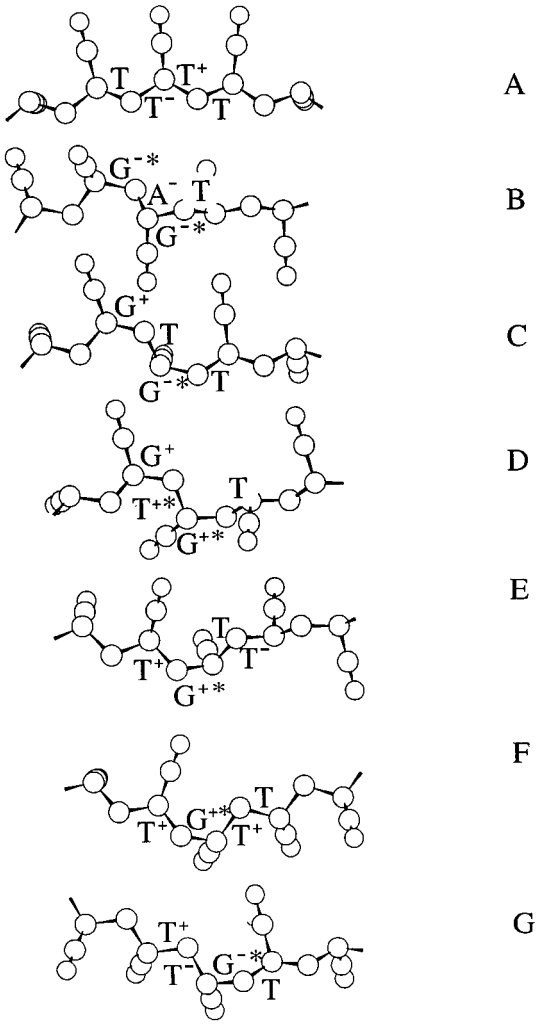

Figure 8. Side views of the chain stretches, with an isolated *mm* triad between *r* diads, in the minimum energy conformations: (A) TT⁻|T⁺T, (B) G⁻*A⁻|G⁻*T, (C) G⁺T|G⁻*T, (D) G⁺T⁺*|G⁺T, (E) T⁺G⁺*|TT⁻, (F) T⁺G⁺*|T⁺T, and (G) T⁺T⁻|G⁻*T (see Table 5).

the thermal factors and the hydrogen atoms were not included in the Fourier transform calculations.

6. Fourier Transform. Results

Figure 9 plots the calculated X-ray diffraction intensity (I_c) for an isotactic PAN chain in the minimum energy extended conformation described in Table 3 with $...|\theta_1\theta_1|\theta_2\theta_2|... = ...|T^+T^+*|T^-*T^-|...$ along the meridian (i.e. at $\xi = 0$, Figure 9A) and in the ξ, ζ projection, in the form of curves with a constant value of I_c (Figure 9B).

Parts C and D of Figure 9 are the analogous I_c plots for a syndiotactic PAN chain, in the *trans*-planar minimum energy conformation.

The presence of two peaks close to $\zeta \approx 0.4$ Å^{-1} and 0.8 Å^{-1} is apparent along the meridian (Figure 9A,C) for both tacticities. The calculated diffraction intensity map for syndiotactic PAN (Figure 9D) shows, beside the meridional peaks, the presence of a halo centered at $\xi \approx 0.15$ Å^{-1} and $\zeta \approx 0.20$ Å^{-1}, which is absent for the isotactic model chain. As already noted by Liu and Ruland in ref 9, the experimental intensity distribution outside of the equator (Figure 3) exhibits qualitative similarity with the calculated pattern for the syndiotactic PAN chain in the *trans*-planar conformation (Figure 9D).

Substantial differences exist, however, between the experimental (Figure 2) and calculated (Figure 9C) meridional profiles. In particular, the calculated patterns of the stereoregular extended chains do not account for the diffuse nature of the scattering along the meridian in the experimental pattern. We notice that the halo at $\zeta \approx 0.3$ Å^{-1}, which is present in the experimental profile (Figure 2), does not need to be considered since it is only a tail of the halo at $\xi \approx 0.15$ Å^{-1} and $\zeta \approx 0.25$ Å^{-1}, reinforced by the imperfect alignment of the chains with the fiber axis (see Figure 3).

Figure 10 shows the calculated X-ray diffraction intensity in the ξ, ζ projection (Figure 10A) and along the meridian (Figure 10B), for atactic decamers of PAN including 50% of *m* diads in the *trans*-planar conformation. We notice that the calculated pattern of these atactic, but still extended, model chains does not account for the diffuse nature of the scattering along the meridian nor does it accounts for the position of the meridional maxima in the experimental pattern. From an inspection of Figure 10A, it is apparent that a prevalent syndiotactic configuration is not necessary to account for the presence of a halo centered at $\xi \approx 0.15$ Å^{-1} and $\zeta \approx 0.20$ Å^{-1}.

Figure 11 shows the calculated X-ray diffraction intensity in the ξ, ζ projection (Figure 11A) and along the meridian (Figure 11B), averaged over eight different model atactic stretches of PAN, including the conformations of Table 5, comprising a G* correspondingly to the *m* diads, which shorten the mean chain periodicity, as an example. The profiles of parts C and D of Figure 11 (or 10) are calculated along the meridian, including the CN groups alone and the backbone carbon atoms alone, respectively. It is worth noting that the meridional profiles show a halo centered at $\zeta = 0.42$ Å^{-1} in Figure 11C (at $\zeta = 0.39$ Å^{-1} in Figure 10C) and a halo centered at $\zeta = 0.78$ Å^{-1} in Figure 11D (and Figure 10D). This indicates that in the profile of Figure 11B (Figure 10B) the maximum at $\zeta = 0.78$ Å^{-1} is not necessarily the second-order diffraction of the maximum at ζ around 0.40 Å^{-1}, since they may originate from different contributions. In comparing Figure 11A−D with Figure 10A−D, it is worth noting that the inclusion of the conformations, implying locally large deviations from the *trans*-planar conformations, produces, in better qualitative agreement with experimental data, a shift of the first maximum to $\zeta = 0.42$ Å^{-1} whereas the

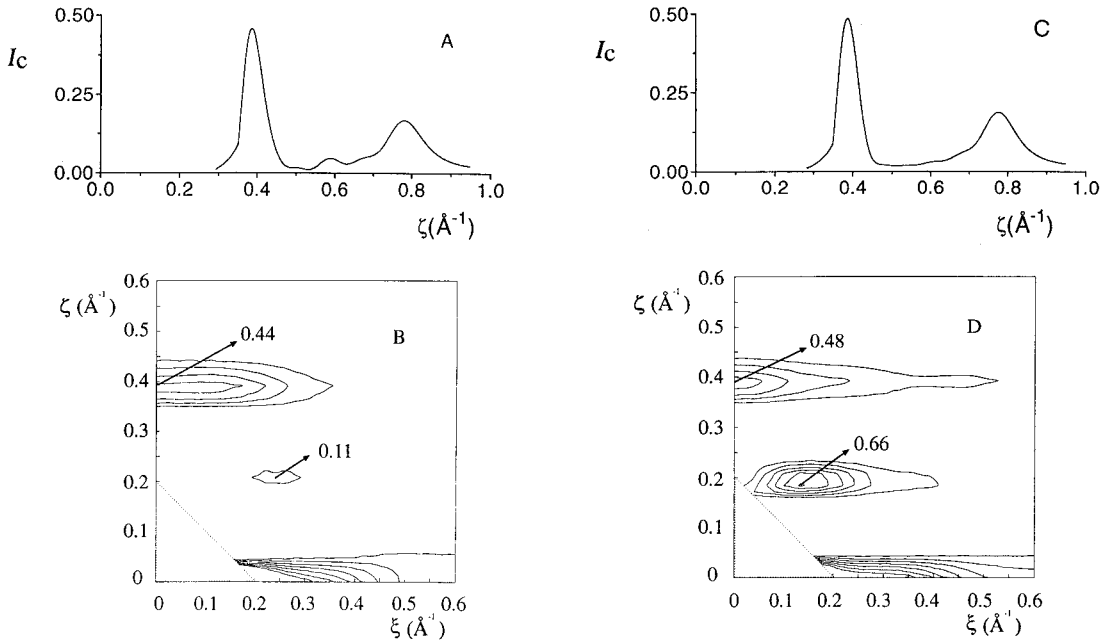

Figure 9. Calculated diffraction intensity (uncorrected for the polarization and the absorption, in arbitrary units) $I_c(\xi,\zeta)$ for isotactic (A, B) and syndiotactic (C, D) chains of PAN. (A, C). Plots along the meridian, i.e. for $\xi = 0$. (B, D). Intensity vs coordinates ξ and ζ. Contour lines correspond to the values 0.1, 0.2, 0.3, 0.4, and 0.5. The chain conformation for the isotactic configuration corresponds to the minimum energy extended chain conformation of Table 3 with $...|\theta_1\theta_1|\theta_2\theta_2|... = ...|T^+T^+*|T^-*T^-|....$

position of the second maximum remains unaltered around 0.80 Å^{-1}, the broadening of the meridional maxima, and a net reduction of the ratio between the maximum heights of these two meridional haloes. We also notice that in Figure 11A, in accord with the experimental observations, the diffuse scattering off the meridian is now centered at $\xi \approx 0.15$ Å^{-1} and $\zeta \approx 0.26$ Å^{-1}. Hence, this maximum may be shifted toward higher ζ values with respect the syndiotactic chains, for the presence of the conformational disorder.

In summary, the present analysis indicates that the paracrystalline pseudohexagonal phase of PAN is formed by short and straight chain stretches, with atactic configuration. Although a nearly *trans*-planar conformation for configurationally irregular chains could be possible at a cost of conformational energy which can be afforded at least locally, corresponding to chains with mean periodicity of nearly 2.5 Å (see Tables 4 and 5), for *mm* diads (or for longer *m* sequences) also extended conformations with large deviations of backbone dihedral angles from 180° are energetically feasible. An interesting feature of such conformations is that they comprise locally dihedral angles in a G* state within *m* sequences. The latter and analogous conformations for longer isotactic sequences are able to reduce the mean periodicity along the chain axis (Table 5) to values compatible with the experimental density values, thus providing a possible description of the kinked regions along the chains which were postulated by Liu and Ruland.[9]

It is worth noting that the good agreement with the experimental diffraction pattern of the calculated patterns indicates that there is no long-range order in the relative shift of the chains along *z*; in other words, only very short-range order in the relative shift of the chains along *z* is compatible with the experimental pattern.

7. Conclusions

In this paper, we have examined the various kinds of physical order (at the molecular level) which are present in drawn fibers of polyacrylonitrile.

From the chemical point of view, in acrylonitrile polymers, which are produced industrially, there is substantial constitutional (head-to-tail) order in the succession of units along the macromolecular chains but almost complete disorder in the succession of the *m* and *r* relative configurations of the tertiary backbone carbon atoms.

This notwithstanding, the X-ray diffraction patterns of polyacrylonitrile fibers show the characteristic features of positional order at intervals of distances, which range from short to long. The main points that we have contributed to clarify in this paper and the corresponding conclusions are the following.

(1) Hexagonal Long-Range vs Orthorhombic Shorter Range. In polyacrylonitrile fibers, there is no long-range order for the position of the (individual) chain carbon atoms; there is long-range order, instead, in the positioning of the chain axes. The chain axes are arranged in a hexagonal array ($a = b = 6.0$ Å, $\gamma = 120°$) for equatorial distances (along *a* and *b*) on the order of magnitude of 100 Å; the chains are almost fully extended, yet configurationally and conformationally disordered, with a mean repetition period $c = \sim 2.4$ Å/mu.

It is observed in some preparations [aggregates of single crystals deposited from solutions for electron diffraction (Hinrichsen and Orth[7] as well as our unannealed fibers as drawn, see above and ref 17)] that the hexagonal array may be locally deformed into smaller, orthorhombic arrays (cell with $a = 10.6$ Å, $b = 11.6$ Å, $c \approx 2.5$ Å/mu) at shorter, but still long, equatorial distances (these more ordered arrays are still capable in fact of giving Bragg reflections; see above).

(2) Energetic Feasibility of Extended Conformations for Configurationally Ordered and Disordered Chains. A conformational analysis has allowed location of minimum energy extended conformations for isotactic and syndiotactic model chains of PAN as well as for atactic model chains, comprising isolated *m* diads or *mm* triads, as an example. Syndiotactic model chains, of course, generate minimum energy extended

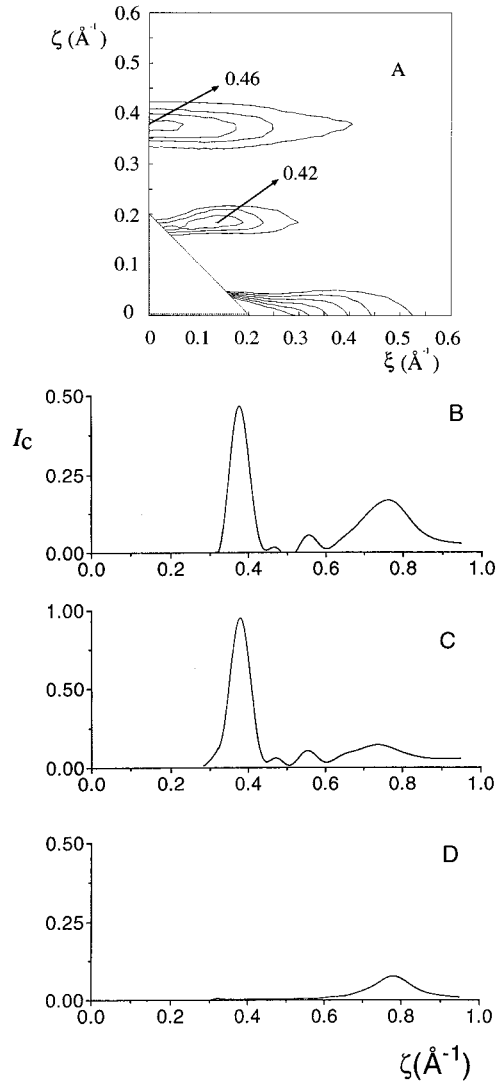

Figure 10. Calculated diffraction intensity (uncorrected for the polarization and the absorption, in arbitrary units) $I_c(\xi,\zeta)$ for a stereoirregular PAN chain, with 50% *m* diads in a nearly *trans* conformation vs the reciprocal coordinates ξ and ζ (A) and the corresponding plot along the meridian up to $\zeta = 0.95$ Å^{-1} (B). In A, contour lines correspond to 0.1, 0.2, 0.3, 0.4, and 0.5. The scattering along the meridian arises from CN groups only (C) and from the backbone carbon atoms only (D).

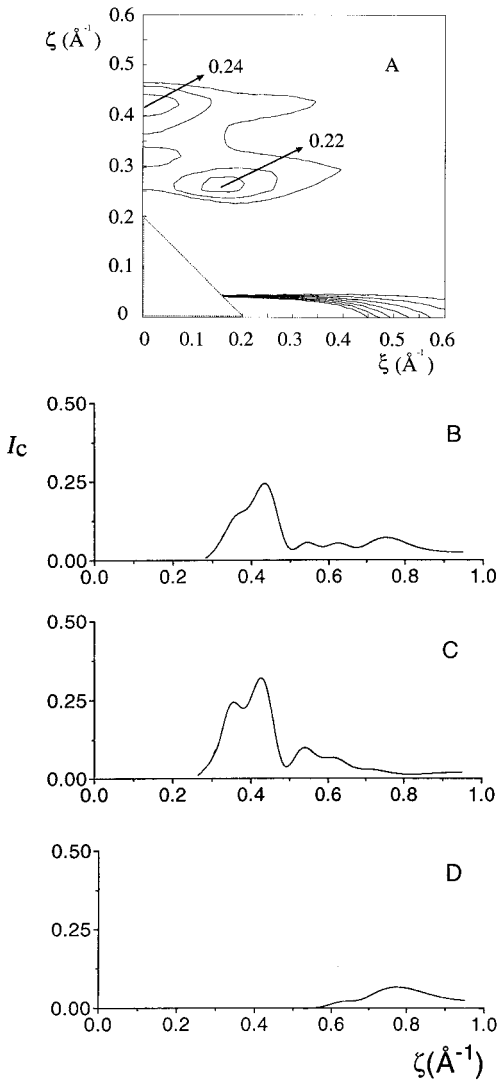

Figure 11. Calculated diffraction intensity (uncorrected for the polarization and the absorption, in arbitrary units) $I_c(\xi,\zeta)$ for a stereoirregular PAN chain, with 50% *m* diads and including the conformations listed in Table 5 shortening the mean chain periodicity (comprising a G*), averaged over at least eight different chain models vs the reciprocal coordinates ξ and ζ (A) and the corresponding plot along the meridian up to $\zeta = 0.95$ Å^{-1} (B). In A, contour lines correspond to 0.05, 0.1, 0.15, and 0.20. The scattering along the meridian arises from CN groups only (C) and from the backbone carbon atoms only (D).

all-trans conformations with a periodicity close to 2.5 Å. Isolated *m* diads as well as *mm* triads are easily accommodated in extended chains suitable for the crystalline regions of PAN in several minimum energy conformations, implying also large deviations from the *trans* state close to the *m* diads and hence shortening significantly the mean periodicity (in the range 2.4-2.3 Å). Among these conformations we remark on those comprising dihedral angles in the G* state corresponding to a *m* diad, which are suitable also for isotactic sequences longer than the triads. These conformers project perpendicularly to the chain axis with CN groups pointing along directions which are displaced from each other by roughly 120°.

(3) X-ray Diffraction Profiles Calculations. The Fourier transform of PAN model chains have been calculated and the results, compared to the experimental X-ray diffraction data, indicate the following.

(i) The inclusion in the pseudohexagonal phase of PAN of conformers even with dihedral angles displaced from 180° (corresponding to *m* diads) does not shorten much the mean periodicity of the chain; preliminary calculations of the diffraction patterns on chains with disordered configuration and extended but disordered conformation are in agreement with the diffuse scattering along the meridian and provide an explanation for the presence in the meridional profile of broad diffraction maxima around $\zeta = 0.80$ and 0.42 Å^{-1}. This last maximum is mainly due to the scattering along ζ of CN groups while the maximum at $\zeta = 0.80$ Å^{-1}, instead, mainly comes from the scattering along ζ of the backbone carbon atoms.

(ii) A predominantly syndiotactic chain is not necessary to get nonnegligible diffuse scattering off the meridian centered at $\xi \approx 0.15$ Å^{-1} and $\zeta \approx 0.20$ Å^{-1}: the intensity of this halo is still strong with respect to the case of the fully syndiotactic model chain, for atactic stretches of PAN in those conformations shortening the chain length and with CN groups projecting perpendicular to the chain axis at 120° from each other.

(iii) While there is long-range order in the positions of the chains, there is only a very short-range order in the relative shift of the chains along *z* and only local orientational order of CN groups possibly directed along the lattice directions *a*, *b*, and $-(a + b)$; a waviness of the atactic PAN stretches may comply more easily with the local packing of CN groups.

According to our analysis, the low energy extended conformations discussed previously for configurationally disordered model chains of PAN, are able to account for the experimental diffraction patterns as well as for the experimental density value. In other words, in contrast to the work of Hinrichsen and Orth[7] and Liu and Ruland,[9] the crystallizable stretches should not be necessarily syndiotactic. This gives a possible explanation, in terms of local conformations, of the crystallizability of PAN despite of the large configurational disorder.

Thus, the disorder present in PAN crystals should be classified in the second of the three categories considered in a previous paper by two of us:[32] the PAN crystals have long-range positional order only for a structural feature that is not point-centered, that is, for the chain axes, for which the two $a = b$ periodicities are sufficient to define a three-dimensional repetition.

The PAN crystals can be also considered in the category of stiff conformationally disordered (condis) crystals as defined by Wunderlich et al.,[33] if we expand their definition to include cases of conformational disorder as arising from built-in configurational disorder (and not from a thermodynamic transition); the disordered (though extended) conformations, probably frozen at room temperature, may undergo rapid, dynamic changes above the temperature associated with the α_{II} relaxation, as described by Minami[34] and some of us.[17]

Acknowledgment. The authors thank Dr. Raffaele Tedesco of the Montefibre SpA, of Porto Marghera, for useful discussions. This work was supported by the Ministero dell'Università e della Ricerca Scientifica e Tecnologica (Italy) and by the Consiglio Nazionale delle Ricerche. X-ray diffraction data were recorded with a Nonius CAD4 automatic diffractometer (Centro Interdipartimentale di Metodologie Chimico Fisiche, University of Naples).

References and Notes

(1) Natta, G.; Mazzanti, G.; Corradini, P. *Atti Accad. Naz. Lincei, Cl. Sci. Fis., Mat. Nat., Rend.* **1958**, *25*, 3.
(2) Stefani, R.; Chevreton, M.; Garnier, M.; Eyraud, C. *Compt. Rend.* **1960**, *251*, 2174.
(3) Bonh, C. R; Schaefgen, J. R.; Statton, W. O. *J. Polym. Sci.* **1961**, *55*, 531.
(4) Holland, V. F.; Mitchell, S. B.; Hunter, W. L.; Lindenmeyer, P. H. *J. Polym. Sci.* **1962**, *62*, 145.
(5) Lindenmeyer, P. H.; Hosemann, R. *J. Appl. Phys.* **1963**, *34*, 42.
(6) Klement, J. J.; Geil, P. H. *J. Polym. Sci. A-2* **1968**, *6*, 1381
(7) Hinrichsen,G.;Orth, H. *Kolloid-Z. Z. Polym.* **1971**, *247*, 844.
(8) Colvin, B. G.; Storr, P. *Eur. Polym. J.* **1974**, *10*, 337.
(9) Liu, X. D.; Ruland, W. *Macromolecules* **1993**, *26*, 3030.
(10) Hobson, R. J.; Windle, A. H. *Polymer* **1993**, *34*, 3582.
(11) Hobson, R. J.; Windle, A. H. *Macromolecules* **1993**, *26*, 6903.
(12) Schaefer, J. *Macromolecules* **1971**, *4*, 105.
(13) Kamide, K.; Yamazaki, H.; Okajiama, K.; Hikichi, K. *Polym. J.* **1985**, *17*, 1233.
(14) Kamide, K.; Yamazaki, H.; Okajiama, K.; Hikichi, K. *Polym. J.* **1985**, *17*, 1291
(15) Stefani, R.; Chevreton, M.; Terrier, J.; Eyraud, Ch. *Compt. Rend.* **1959**, *248*, 2006.
(16) Chiang, J. *J. Polym.Sci. A*, **1963**, *1*, 2765; **1965**, *3*, 2109.
(17) Rizzo, P.; Guerra, G.; Auriemma, F. *Macromolecules* **1996**, *29*, 1830
(18) Hinrichsen and Orth in ref 7 observed in some aggregates of single crystals deposited from solutions for electron diffraction that the hexagonal array of PAN may be locally deformed into smaller, orthorhombic arrays (cell with $a = 10.6$ Å, $b = 11.6$ Å, $c \approx 2.5$ Å/mu) the equatorial correlation dimensions of which are big enough to be capable of giving Bragg reflections. There is probably some local orientational order of the CN groups, at least for space filling reasons. The CN groups could alternate along two preferred directions in the orthorhombic locally ordered portions and along the lattice directions *a*, *b*, $-(a + b)$ for the hexagonal lattice. It is worth noting that the local orientational and positional correlation of the lateral CN groups would be similar as those observed for chlorine atoms in crystals of PVC corresponding to a syndio- or a syndio-emulating structure (see refs. 10 and 20).
(19) Natta, G.; Corradini, P. *J. Polym. Sci.* **1956**, *20*, 251. Wilkes, C. E.; Folt, V. L.; Krimm, S. *Macromolecules* **1993**, *6*, 235. Hobson, R. J.; Windle, A. H. *Macromol. Chem Theory Simul.* **1993**, *2*, 263.
(20) Hennico, G.; Delhalle, J. *J. Chem. Soc. Faraday Trans.* **1990**, *86*, 1025.
(21) Yamadera, R.; Tadokoro, H.; Murahashi, S. *J. Chem. Phys.* **1964**, *41*, 1233.
(22) Vacatello, M.; Flory, P. J. *Macromolecules* **1986**, *19*, 405.
(23) Petraccone,V.; Pirozzi, B; Frasci, A.; Corradini,P. *Eur. Polym. J.* **1976**, *12*, 323
(24) Ooi, T.; Scott, R. A.; Vanderkooi, G.; Sheraga, H. A. *J. Chem. Phys.* **1967**, *46*, 4410.
(25) Sundararajan, P. R.; Flory, P. J. *J. Am. Chem. Soc.* **1974**, *96*, 5025.
(26) Henrici-Olivè, G.; Olivè, S. *Adv. Polym. Sci.* **1979**, *32*, 125.
(27) IUPAC Commission on Macromolecular Nomenclature *Pure & Appl. Chem.* **1980**, *53*, 733.
(28) Corradini, P. In *The Stereochemistry of Macromolecules*; A. D. Ketley, Ed.; Marcel Dekker: New York, 1968.
(29) Cavallo L.; Corradini P., private communication. See also Figure 4C,B of Corradini (Corradini, P. *Macromol. Chem., Macromol. Symp.* **1993**, *66*, 1124) showing models of highly extended conformations (average periodicity per monomeric unit ≥2.5 Å) for polymorphic modifications of both syndiotactic *and isotactic* polystyrene.
(30) Tadokoro, H. *Structure of Crystalline Polymers*; J. Wiley & Sons: New York, 1979
(31) Auriemma, F; Petraccone, V.; Dal Poggetto, F.; De Rosa, C.; Guerra, G.; Manfredi, C.; Corradini, P. *Macromolecules* **1993**, *26*, 3772
(32) Corradini, P.; Guerra, G. *Adv. Polym. Sci.* **1992**, *100*, 183.
(33) Wunderlich, B.; Möller, M.; Greebowicz, J.; Baur, H. *Adv. Polym. Sci.* **1988**, *87*, 1
(34) Minami, S. *Appl. Polym. Symp.* **1974**, *25*, 145.

MA960699M